ECT*-05-06; CERN-PH-TH-2005-143; SPhT-T05/126; TIFR/TH/05-30

Elliptic flow and incomplete equilibration at RHIC

Rajeev S. Bhalerao,[1] Jean-Paul Blaizot,[2] Nicolas Borghini,[3] and Jean-Yves Ollitrault[4]

[1]*Department of Theoretical Physics, TIFR, Homi Bhabha Road, Colaba, Mumbai 400 005, India*
[2]*ECT*, Villa Tambosi, strada delle Tabarelle 286, I38050 Villazzano (TN), Italy*
[3]*Physics Department, Theory Division, CERN, CH-1211 Geneva 23, Switzerland*
[4]*Service de Physique Théorique, CEA/DSM/SPhT, Unité de recherche associée au CNRS, F-91191 Gif-sur-Yvette Cedex, France.*

(Dated: February 14, 2014)

We argue that RHIC data, in particular those on the anisotropic flow coefficients v_2 and v_4, suggest that the matter produced in the early stages of nucleus-nucleus collisions is incompletely thermalized. We interpret the parameter $(1/S)(dN/dy)$, where S is the transverse area of the collision zone and dN/dy the multiplicity density, as an indicator of the number of collisions per particle at the time when elliptic flow is established, and hence as a measure of the degree of equilibration. This number serves as a control parameter which can be varied experimentally by changing the system size, the centrality or the beam energy. We provide predictions for Cu–Cu collisions at RHIC as well as for Pb–Pb collisions at the LHC.

PACS numbers: 25.75.Ld, 24.10.Nz

The observation of azimuthal anisotropy in the production of particles in ultra-relativistic nucleus-nucleus collisions, especially the so-called elliptic flow v_2 [1], is one of the highlights of the RHIC heavy ion program [2, 3]. The phenomenon, first identified in this regime at the CERN SPS [4], reflects the anisotropy of the region of overlap of the nuclei and is a direct consequence of the reinteractions between the produced particles. In the limit where the collisions are frequent enough to drive the system quickly to local equilibrium, fluid dynamics provides an intuitive physical explanation for the origin of anisotropic flow: particles tend to go in the direction of the strongest pressure gradients, hence preferably in the collision plane [5]. Of course, local equilibrium is not a necessary condition for elliptic flow, but it is commonly accepted that deviation from equilibrium can only reduce the magnitude of the effect.

In fact, the main characteristics of the observed elliptic flow are reasonably well described by ideal fluid dynamics [6], while requiring unreasonably large cross sections in transport models [7, 8]. The ability of the former to reproduce both the elliptic flow and single-particle spectra for measured hadrons with $p_T \lesssim 2$ GeV/c near midrapidity in minimum-bias collisions is considered a significant finding at RHIC; by contrast, at the SPS a simultaneous fit of both observables appears impossible. The dependence of the flow pattern on hadron masses further supports the hydrodynamical picture. Very strong conclusions have been drawn from this apparent success [9]: one argues that local equilibrium has to be established on short time scales (~ 0.6 fm/c [6]) while viscosity should be negligible, suggesting a "perfect fluid" behaviour for the created matter [10].

In this Letter we would like to question these conclusions. On the one hand, the short time scale for equilibration is difficult to account for microscopically [11] (although it has been argued recently that plasma instabilities may provide a mechanism for fast thermalization; see, e.g., Refs. [12, 13]). On the other hand, several features of the data clearly signal the breakdown of the hydrodynamical description and are more naturally understood if the constraint of local equilibrium is relaxed. Thus, the point of view that we shall adopt here is that matter produced at RHIC is not fully equilibrated, and we shall explore the consequences of such an assumption. As we shall see, this leads to simple predictions that can be easily tested.

This Letter is organized as follows: We first recall the essential features of the elliptic flow using an ideal hydrodynamic picture. We then show that incomplete thermalization leads to specific deviations from hydrodynamical behaviour: these concern in particular the dependence of moments v_2 and v_4 of the azimuthal distribution on the system size and the collision centrality. Note that throughout this paper, we shall only consider the average values of v_2 and v_4 over all particles at a given rapidity; the effects of partial thermalization on the elliptic flow of identified particles, in particular its p_T-dependence, have been discussed in Ref. [14].

Elliptic flow originates from the anisotropy of the initial matter distribution. In hydrodynamics, the dependences of the elliptic flow on the system size and the centrality are essentially determined by the spatial eccentricity, defined as

$$\epsilon = \frac{\langle y^2 - x^2 \rangle}{\langle y^2 + x^2 \rangle}, \tag{1}$$

where x and y are coordinates in the plane perpendicular to the collision axis (with the x-direction in the collision plane, and the origin midway between the centers of the two nuclei). Angular brackets $\langle\cdot\rangle$ denote an average weighted with the initial entropy density $s(x, y)$ (at a given rapidity).

Elliptic flow develops gradually in the system as it evolves. If the speed of sound c_s is constant, the natural time scale is of the order of $\bar{R}/c_s$, where $\bar{R}$ is a measure

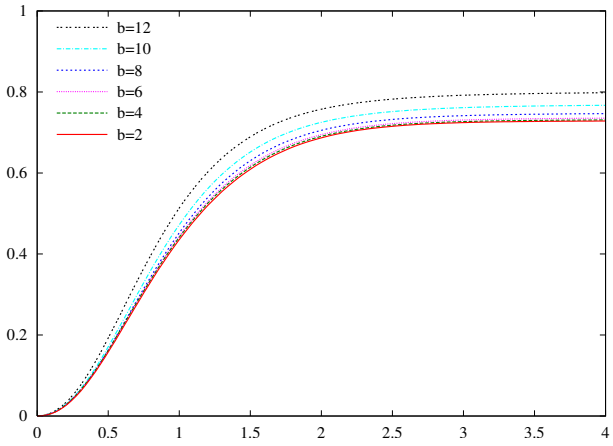

FIG. 1: (Color online) v_2/ϵ as a function of $c_s(t-t_0)/\bar{R}$ for various impact parameter values of Au–Au collisions at $\sqrt{s_{NN}} = 200$ GeV with $c_s = c/\sqrt{3}$.

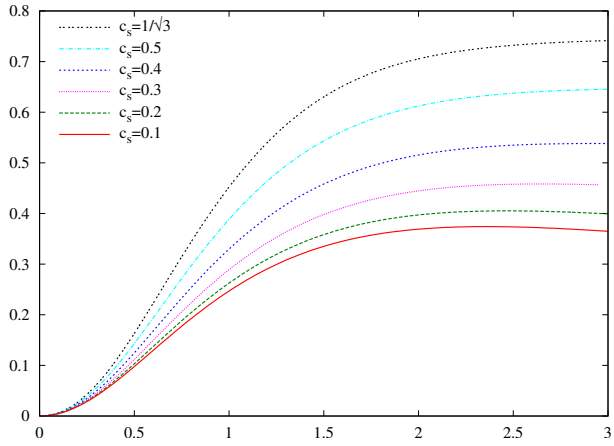

FIG. 2: (Color online) v_2/ϵ as a function of $c_s(t-t_0)/\bar{R}$ for various values of c_s in the case of Au–Au collisions at $\sqrt{s_{NN}} = 200$ GeV with impact parameter $b = 8$ fm.

of the transverse size of the system: the anisotropy of the momentum distributions can be fully achieved only once all parts of the system are "informed" about the initial spatial anisotropy, and that takes a time of the order of $\bar{R}/c_s$. We define $\bar{R}$ through $1/\bar{R} = \sqrt{1/\langle x^2\rangle + 1/\langle y^2\rangle}$ (since flow is an effect of pressure *gradients*, $\bar{R}$ is a more natural choice than, e.g., the rms radius).

Hydrodynamical results are presented in Fig. 1, which displays the time evolution of elliptic flow (i.e., the value of v_2 that one would observe if the system was to decouple at time t) for various centralities. The procedure is detailed in Ref. [5]. There, v_2 is defined as $v_2 \equiv \langle p_x^2 - p_y^2\rangle/\langle p_x^2 + p_y^2\rangle$, where average values are taken over all particles. This yields values of v_2 that are typically a factor 2 larger than those obtained with the more conventional definition, $v_2 \equiv \langle (p_x^2 - p_y^2)/(p_x^2 + p_y^2)\rangle$. The longitudinal expansion is assumed boost-invariant; the hydrodynamical evolution starts at a time $t_0 = 0.6$ fm/c after the collision. We checked that the results are independent of the value of t_0 as long as t_0 is much smaller than $\bar{R}/c_s$. In line with the discussion above, we have plotted v_2 divided by ϵ, and the elapsed time $t - t_0$ divided by the characteristic time $\bar{R}/c_s$. This results in an almost perfect scaling for a large range of impact parameters (from $b = 2$ to $b = 12$ fm) for which the eccentricity varies by more than one order of magnitude and $\bar{R}$ by a factor 2 (see Table I below). Note, in particular, that the final value of v_2 is independent of the system size ($\bar{R}$) for a given shape (ϵ). This is a consequence of the scale invariance of ideal fluid dynamics.

The magnitude of v_2 also depends on the fluid properties, in particular on the speed of sound c_s. In order to illustrate this dependence, we have repeated the calculation for various values of c_s. The results are presented in Fig. 2. When c_s is large enough ($c_s \gtrsim 0.3$), v_2 is proportional to c_s. This no longer holds when c_s becomes small ($c_s \lesssim 0.2$): in this "nonrelativistic" regime, the expansion of the system is entirely controlled by the dimensionless parameter $c_s(t-t_0)/\bar{R}$: we have checked that v_2/ϵ becomes a universal curve for $c_s < 0.1$. Note that the results plotted in Fig. 2 have been obtained by assuming that c_s is constant throughout the evolution. In the real world, c_s varies. In particular, if the system enters a regime where the equation of state is soft, i.e., where the speed of sound is small, the resulting v_2 may be significantly reduced [15].

In summary, we have seen that within ideal fluid dynamics the final value of the elliptic flow v_2 is proportional to the initial spatial eccentricity ϵ [5], is independent of the system size $\bar{R}$, grows with the speed of sound c_s, and has a characteristic build-up time $\sim \bar{R}/c_s$. Note that this time scale for the build-up of the elliptic flow is of the same order of magnitude (although somewhat larger) in transport calculations (see, e.g., Refs. [8, 16]).

We start now exploring the consequences of incomplete equilibration. To do so, we characterize the degree of thermalization by a dimensionless parameter, the Knudsen number K [17]. By definition, K^{-1} is the typical number of collisions per particle. Local thermal equilibrium is achieved if $K^{-1} \gg 1$. We are going to show that K^{-1} can be determined from the data, as it is proportional to $(1/S)\, dN/dy$, where dN/dy is the total multiplicity density, while $S \equiv 2\pi\sqrt{\langle x^2\rangle\langle y^2\rangle}$ is a measure of the transverse area of the collision zone (with this definition of S, which is larger by a factor 2 than that adopted in Ref. [4], $(1/S)\, dN/dy$ is the maximum value of the density for a Gaussian density distribution).

The relevant length and time scales for elliptic flow are $\bar{R}$ and $\bar{R}/c_s$, respectively. Therefore, the typical number of collisions per particle is given by $\bar{R}/\lambda$, where λ is the mean free path at time $\bar{R}/c_s$. This mean free path λ depends on the particle density n: $1/\lambda = \sigma n$, with σ a cross section characterizing the interactions among the produced particles. The particle density, in turn, depends on time. We assume that the total particle number is conserved throughout the evolution: this is justified

TABLE I: Parameters for Au–Au collisions at $\sqrt{s_{NN}} = 200$ GeV. See text for details.

b (fm)	ϵ	$\bar{R}$ (fm)	$\frac{dN}{dy}$	$\frac{1}{S}\frac{dN}{dy}$ (mb^{-1})	$n\left(\frac{\bar{R}}{c_s}\right)$ (fm^{-3})
0	0	2.07	1050	1.95	5.4
2	0.033	2.02	975	1.90	5.4
4	0.115	1.89	790	1.77	5.5
6	0.215	1.68	562	1.55	5.3
8	0.315	1.45	344	1.23	4.9
10	0.398	1.22	167	0.82	3.8
12	0.433	1.04	55	0.37	2.0

TABLE II: Parameters for Cu–Cu collisions at $\sqrt{s_{NN}} = 200$ GeV

b (fm)	ϵ	$\bar{R}$ (fm)	$\frac{dN}{dy}$	$\frac{1}{S}\frac{dN}{dy}$ (mb^{-1})	$n\left(\frac{\bar{R}}{c_s}\right)$ (fm^{-3})
0	0	1.42	275	1.09	4.5
2	0.043	1.36	240	1.02	4.3
4	0.141	1.23	159	0.83	3.9
5.5	0.216	1.10	95	0.61	3.2
6	0.237	1.06	77	0.53	2.9
8	0.265	0.93	22	0.20	1.2

by the observation that n is proportional to the entropy density, and that entropy is conserved. This allows us to estimate the particle number density at time τ from the relation

$$c\tau n(\tau) \sim \frac{1}{S}\frac{dN}{dy}, \tag{2}$$

valid for times $\tau \lesssim \bar{R}/c_s$, i.e., as long as the transverse size of the system does not vary significantly. One eventually obtains

$$K^{-1} = \frac{\bar{R}}{\lambda} = \bar{R}\,\sigma\, n\left(\frac{\bar{R}}{c_s}\right) = \frac{\sigma}{S}\frac{dN}{dy}\frac{c_s}{c}. \tag{3}$$

Tables I and II provide numerical values of $(1/S)\,dN/dy$ for two colliding systems, Au–Au and Cu–Cu, at the same center-of-mass energy $\sqrt{s_{NN}} = 200$ GeV. They are given in mb^{-1}, making the conversion into a Knudsen number easy once the cross section is known (up to a factor c_s/c). With a typical partonic cross section of 3 mb, and a speed of sound $c_s \sim c/\sqrt{3}$, one thus finds $K^{-1} \simeq 2$ for a semi-central Au–Au collision. This is not much larger than unity, and the ideal fluid limit probably requires larger cross sections, as already inferred from transport calculations. The Knudsen number can also be estimated from the viscosity [18], with similar conclusions.

Incomplete equilibration breaks the scale invariance of ideal fluid dynamics: v_2 depends on the system size $\bar{R}$ through K^{-1}. As K^{-1}, increases, the magnitude of v_2 grows linearly—the larger the number of collisions, the larger the momentum anisotropy—, eventually saturating when the system reaches local equilibrium. To fix ideas, one may have in mind the following simple formula, which exhibits the correct qualitative behaviour:

$$v_2 = v_2^{\rm hydro}\frac{K^{-1}}{K^{-1} + K_0^{-1}}\,, \tag{4}$$

where $v_2^{\rm hydro}$ is the value of v_2 obtained from hydrodynamics, i.e., corresponding to the large K^{-1} limit, and K_0^{-1} is a number of order unity, whose precise value can only be determined through an explicit transport calculation. Referring to the transport calculations in Ref. [16], one finds only a modest increase of v_2 (by 40%) when σ increases from 3 to 10 mb, K^{-1} from 2 to 7, which corresponds to $K_0^{-1} \simeq 1.5$.

We are now in position to examine whether the matter produced at RHIC is in local equilibrium. To do so, we need to vary the value of K^{-1}. This can be done by changing the system size $\bar{R}$, while keeping the mean free path λ constant [see Eq. (3)]. Since λ depends on the density (explicitly, and through a potential dependence of the cross section on the density), this requires keeping the density constant. Now, the last column of Table I shows that the particle density remains approximately constant in Au–Au collisions for a large range of impact parameters, between central events and collisions with $b = 8$ fm. In this case, K^{-1} is then proportional to the system size $\bar{R}$ or, equivalently, to $(1/S)\,dN/dy$ [see Eq. (3)]. For small K^{-1}, we expect from Eq. (4) that v_2/ϵ is proportional to K^{-1} (since $v_2^{\rm hydro}$ scales like ϵ), i.e., that v_2/ϵ scales like $(1/S)\,dN/dy$. Indeed, such a linear variation was found in Ref. [4] (see Fig. 25), for both the RHIC Au–Au values and the SPS Pb–Pb values. It even turns out that both linear dependences match well, although the densities differ (the densities at SPS are typically 40% smaller than at RHIC), which suggests that the cross section (and c_s) used in estimating the Knudsen number can be taken as roughly constant across the different beam energies.

We take the above-mentioned plot in Ref. [4] as evidence that local equilibrium is not achieved, since v_2/ϵ is steadily increasing with $(1/S)\,dN/dy$, without any hint at a saturation, for the whole accessible experimental range. A similar evidence comes from the variation of v_2 with pseudorapidity η [19, 20]: changing the latter induces a variation of the multiplicity density $dN/d\eta$, hence of the control parameter at fixed geometry, which is reflected in $v_2(\eta)$. Finally, the decrease in the number of collisions as the transverse momentum increases also results in a departure from equilibrium seen on $v_2(p_T)$ data [14], and in transport calculations [8]. In the latter, for the bulk of the particles ($p_T \lesssim 500$ MeV/c), v_2 already saturates for σ of the order of 3 mb. For higher values of p_T, the saturation occurs only above 10 mb. Surprisingly, however, the saturation value is significantly below that given by hydrodynamical computations, which calls for further investigation of the discrepancy.

One can also study the effect of incomplete equilibration on the fourth moment v_4. Repeating the same arguments as for v_2, one expects that the behaviour of v_4 as a function of K^{-1} is given, at least qualitatively, by

an equation similar to (4). From the simple observation that both v_2 and v_4 are proportional to K^{-1} for small K^{-1}, one expects that v_4/v_2^2 *decreases* with K^{-1}, reaching a minimum when the hydrodynamical regime is reached. Since it was shown in Ref. [21] that ideal fluid dynamics yields $v_4/v_2^2 = 1/2$ (a similar value was found in Ref. [22] within a specific hydrodynamical model), one expects the ratio to be larger than 1/2 if the system is not fully equilibrated, in agreement with the experimental finding $v_4/v_2^2 \sim 1.2$ [2].

Further predictions can be made to test the assumption of incomplete thermalization. In particular, studying smaller systems at the same center-of-mass energy, where the density is roughly the same (compare Tables I and II), one can obtain direct information on the dependence of v_2/ϵ on the number of collisions per particle, K^{-1}. Consider, e.g., Cu–Cu collisions at $b = 5.5$ fm, which corresponds to collisions with the same centrality as Au–Au collisions with $b = 8$ fm [16]. If the hydrodynamical regime were reached, v_2/ϵ would be roughly independent of the system size: from the values of the eccentricities in Table II, one concludes that the values of elliptic flow in Au–Au and Cu–Cu collisions would be then related by $v_2(\mathrm{Cu}) = 0.69\, v_2(\mathrm{Au})$. If, on the contrary, we are far from equilibrium, so that v_2/ϵ is proportional to K^{-1}, instead of constant, then the relationship reads $v_2(\mathrm{Cu}) = 0.34\, v_2(\mathrm{Au})$. This prediction can be completed by an analogous one concerning v_4/v_2^2: as argued before, this quantity is a decreasing function of the number of collisions, hence should be larger in Cu–Cu collisions than it is in Au–Au collisions. Other predictions can be made, regarding the future experiments at LHC: if, as we have argued, the ideal-fluid limit is not reached even in the most central collisions at RHIC, then v_2/ϵ should further increase in Pb–Pb collisions at $\sqrt{s_{NN}} = 5.5$ TeV. In parallel, one can expect that v_4/v_2^2 will decrease, coming closer to 1/2.

The case for early thermalization at RHIC rests on the argument that the v_2 measurements saturate the hydrodynamical limit. However, the latter may well be underestimated. Indeed, the pion data presented in Fig. 36 of Ref. [2] suggest that the measured v_2 in central collisions *overshoots* the value obtained by a hydrodynamical computation, $v_2(\mathrm{data}) > v_2(\mathrm{hydro})$. We know from the above discussion that it is possible to increase the hydrodynamical prediction for v_2 by increasing the speed of sound. Now, in present hydrodynamical calculations, increasing c_s means taking a harder equation of state, and this spoils the agreement with experimental momentum spectra, which require a soft equation of state [6]. It is important to realize that this requirement is closely linked to the assumption that the system is fully thermalized (see [23] for an alternative to 3-dimensional thermalization) and, even more importantly, reaches chemical equilibrium: in a system in chemical equilibrium, there exists a one-to-one relationship between energy per particle (probed by momentum spectra) and density (probed by dN/dy). Although fits to particle ratios by thermal models are usually interpreted as evidence for chemical equilibrium, there is no direct experimental evidence that the particle density in the system obeys the laws of thermodynamics. In fact, as we have seen before, data indicate that *kinetic* equilibrium is not attained at RHIC, which in turn suggests that chemical equilibrium is not attained either. (Even recent hydro calculations, which assume early chemical freeze-out, start with a system in equilibrium [24].) If one drops the assumption of chemical equilibrium, energy per particle and density become independent variables and the transverse momentum spectra no longer constrain the equation of state.

To summarize, relaxing the constraint of chemical equilibrium allows for a natural explanation of RHIC data on elliptic flow. Deviations from local equilibrium lead to a characteristic dependence of observables such as v_2/ϵ and v_4/v_2^2 on the number of collisions, and this can be tested experimentally.

Acknowledgments

We acknowledge the financial support from CEFIPRA, New Delhi, under its project no. 3104-3.

[1] J.-Y. Ollitrault, Nucl. Phys. A **638**, 195c (1998).
[2] J. Adams *et al.* [STAR Collaboration], Phys. Rev. C **72**, 014904 (2005).
[3] S. S. Adler *et al.* [PHENIX Collaboration], Phys. Rev. Lett. **91**, 182301 (2003).
[4] C. Alt *et al.* [NA49 Collaboration], Phys. Rev. C **68**, 034903 (2003).
[5] J.-Y. Ollitrault, Phys. Rev. D **46** 229 (1992).
[6] P. F. Kolb and U. Heinz, in *Quark Gluon Plasma III*, World Scientific (Singapore), p. 634.
[7] D. Molnár and M. Gyulassy, Nucl. Phys. A **697**, 495 (2002) [Erratum-ibid. A **703**, 893 (2002)].
[8] D. Molnár and P. Huovinen, Phys. Rev. Lett. **94**, 012302 (2005).
[9] D. Teaney, J. Lauret, and E. V. Shuryak, nucl-th/0110037.
[10] M. Gyulassy and L. McLerran, Nucl. Phys. A **750**, 30 (2005); E. V. Shuryak, Nucl. Phys. A **750**, 64 (2005).
[11] R. Baier, A. H. Mueller, D. Schiff, and D. T. Son, Phys. Lett. B **502**, 51 (2001); ibid. **539**, 46 (2002).
[12] P. Arnold, J. Lenaghan, G. D. Moore, and L. G. Yaffe, Phys. Rev. Lett. **94**, 072302 (2005).
[13] A. Rebhan, P. Romatschke, and M. Strickland, Phys. Rev. Lett. **94**, 102303 (2005).
[14] D. Teaney, Phys. Rev. C **68**, 034913 (2003)
[15] P. Huovinen, nucl-th/0505036.
[16] L. W. Chen and C. M. Ko, nucl-th/0505044.
[17] M. Knudsen, Ann. Phys. (Leipzig) **28**, 75 (1909); E. M.

Lifshitz and L. P. Pitaevskii, *Physical Kinetics*, Pergamon Press, (Oxford, 1981), page 48.
[18] S. Gupta, hep-ph/0507210.
[19] T. Hirano, Phys. Rev. C **65**, 011901 (2002).
[20] U. W. Heinz and P. F. Kolb, J. Phys. G **30**, S1229 (2004).
[21] N. Borghini and J.- Y. Ollitrault, nucl-th/0506045.
[22] P. F. Kolb, Phys. Rev. C **68**, 031902(R) (2003).
[23] U. W. Heinz and S. M. H. Wong, Phys. Rev. C **66**, 014907 (2002)
[24] T. Hirano and M. Gyulassy, nucl-th/0506049.